Polymer 50 (2009) 5112–5123

Contents lists available at ScienceDirect

Polymer

journal homepage: www.elsevier.com/locate/polymer

The effect of the glass transition temperature on the toughness of photopolymerizable (meth)acrylate networks under physiological conditions

Kathryn E. Smith [a,*], Suzanne S. Parks [b], Michelle A. Hyjek [c], Sara E. Downey [a], Ken Gall [d]

[a] George C. Woodruff School of Mechanical Engineering, Georgia Institute of Technology, 771 Ferst Drive, Atlanta, GA 30332, USA
[b] Department of Bioengineering, Clemson University, 401 Rhodes Research Center, Clemson, SC 29634, USA
[c] Wallace H. Coulter Department of Biomedical Engineering, Georgia Institute of Technology, 313 Ferst Drive, Atlanta, GA 30332, USA
[d] School of Materials Science and Engineering, George C. Woodruff School of Mechanical Engineering, Georgia Institute of Technology, 771 Ferst Drive, Atlanta, GA 30332, USA

ARTICLE INFO

Article history:
Received 5 May 2009
Received in revised form
13 August 2009
Accepted 15 August 2009
Available online 6 September 2009

Keywords:
Toughness
Photopolymerization
Glass transition temperature

ABSTRACT

The purpose of this study is to evaluate how the toughness of photopolymerizable (meth)acrylate networks is influenced by physiological conditions. By utilizing two ternary (meth)acrylate networks, MA-co-MMA-co-PEGDMA and 2HEMA-co-BMA-co-PEGDMA, relationships between glass transition temperature (T_g), water content and state, and toughness were studied by varying the weight ratio of the linear monomers (MA to MMA or 2HEMA to BMA). Differential scanning calorimetry and thermogravimetric analysis were performed to evaluate the thermal behavior and water content as a function of either MA or 2HEMA concentration while tensile strain-to-failure tests were performed at 37 °C to determine network toughness. Both networks exhibited a maximum in toughness in PBS in the composition corresponding to a T_g close to the testing temperature. This toughness maximum was achieved by adjusting the glass transition temperature and/or hydrophilicity through changes in chemistry. These relationships may be utilized to design tough photopolymerizable networks for use in mechanically rigorous biomedical applications.

1. Introduction

A key characteristic of a viable orthopedic biomaterial is its ability to withstand harsh mechanical environments, such as those found in the knee, hip, and spinal regions. First, the mechanical properties of the material (specifically, its modulus) must mimic the mechanical behavior of native orthopedic tissue (i.e. tendon, cartilage, or ligament) in order to avoid a mechanical mismatch between the synthetic material and biological tissue resulting in device failure and injury to adjacent tissue. Second, the material must have excellent toughness to be able to sustain large repeated loading regimes. Several polymer networks have been developed that meet the first mentioned criteria [1–3], but there are only a few reported polymer networks that exhibit excellent toughness [1,2,4]. By enhancing toughness of polymer networks, wear and fatigue failures can be minimized, and the mechanical properties can be better aligned with naturally tough orthopedic soft tissues. Even synthetic degradable polymers, that are intended to dissolve in the body, can benefit from enhanced toughness since premature fracture, wear, or fatigue can greatly affect degradation rate and device performance prior to complete dissolution.

Designing tough, chemically crosslinked polymer networks first requires understanding what chemical characteristics influence the mechanical properties as well as how these structure–property relationships change under physiological conditions. Due to the viscoelastic or viscoplastic nature of polymers, the mechanical properties of polymer networks are dependent on the testing temperature in relation to the glass transition temperature (T_g) of the network such that the elastic modulus will decrease and failure strains will increase as the testing temperature approaches T_g [5]. Above T_g, the elastic modulus will plateau or increase slightly and failure strains will decrease [5,6]. Based on this trend from a brittle to ductile to rubbery state, maximal toughness typically occurs at a testing temperature slightly below or at the polymer's T_g where the chains are becoming more mobile allowing the network to sustain larger strains without losing much strength [7]. Because of this relationship between toughness and temperature, the mechanical properties at body temperature rather than room temperature must be considered for implantation into the body.

Due to the aqueous conditions found within the body, it is also important to consider how saline solution or water influences the mechanical properties of polymer networks. In fact, a critical issue with polymers designed to bear large loads *in vivo* is their loss of

* Corresponding author. Tel.: +1 404 3850624; fax: +1 404 894 9140.
E-mail address: ksmith8@gatech.edu (K.E. Smith).

0032-3861/$ – see front matter © 2009 Elsevier Ltd. All rights reserved.
doi:10.1016/j.polymer.2009.08.040

mechanical properties when exposed to moisture [8,9]. Several studies have identified the role of water in altering the mechanical properties of polymer networks [10–12]. Similar to increasing temperature, immersing a polymer in water leads to a decrease in elastic modulus and an increase in failure strains [13]. This change in stress strain behavior from a brittle to more ductile or rubbery state suggests that T_g is decreasing in solution [12,14,15]. Based on these observations, it is possible that water content can also determine the extent to which toughness is altered in solution and thus, can be one mechanism to which toughness can be enhanced under physiological conditions.

The extent to which T_g decreases in water is governed by the total water content within the network as well as the state of the sorbed water molecules [12,14,16]. In general, the T_g of a polymer network will continuously decrease as water absorption into the network increases, an effect driven by the water–polymer interactions created within the network [10,12,14]. In simplistic terms, water molecules can be found in one of two states within the network, each of which plays its own role in the glass transition behavior of polymers. For water molecules that form hydrogen bonds with polymer chains, the term, "bound water", is used while those water molecules that remain distant from the chains and maintain their mobility to form their own hydrogen-bonded clusters are called "free water" [10,14,17,18]. T_g is affected by bound water in that the hydrogen bonding of water molecules to the polymer chains will result in the formation of a one-phase thermodynamic system that will exhibit a T_g that is dependent upon the T_g's and concentrations of the polymer network and water [19]. Thus, the T_g of the system will continuously decrease as the weight fraction of bound water increases. As might be expected, networks that contain highly polar side groups, such as hydroxyl or amine groups, will readily form hydrogen bonds with water molecules, thus increasing the bound and total water content within the network; whereas, a nonpolar component will create an environment for which it is energetically unfavorable for water molecules to bind [20]. Bulky side groups, such as a phenyl ring or long side chain, will also affect the bound water content by acting act as diffusional barriers and preventing water molecules from entering the network and bonding with hydrophilic components [10,14]. Despite not directly bonding with the network, free water also affects the T_g of polymer networks, particularly more hydrophobic polymers, by increasing the intermolecular distance between the polymer chains, thus disrupting the interchain secondary bonding, including both hydrogen bonding and hydrophobic interactions, and increasing chain mobility [10,14]. Hydrophobic polymers in a glassy state, are affected by free water because the lack of binding sites on the polymer chains results in clustering free water molecules within the network that will subsequently lead to reduced chain rigidity indicative of a more rubbery state [14]. Hydrogels, or extremely hydrophilic polymers will also experience a decrease in T_g with free water [10], but this effect only impacts T_g after the formation of hydrogen bonds with available hydrophilic sites on the polymer has been saturated. Independent of hydrophilicity, changing the crosslinking density of the network will also affect total water content by limiting the mobility of water molecules and reducing the availability of hydrophilic binding sites due to steric hindrance [14,20]. These factors must all be considered when understanding the relationship between network chemistry and T_g under aqueous conditions.

Because the mechanical properties of polymers are temperature-dependent and altered under aqueous conditions, it has been suggested that the toughness of polymer networks will be dependent on this relationship between T_g and water content. In this study, the effect of water content and T_g on toughness is examined in photopolymerizable (meth)acrylate networks. Photopolymerizable networks offer additional advantages as polymeric biomaterials due to their ability to be formed *in situ*, and into complex geometries, rendering them useful for minimally invasive procedures [21,22]. In particular, (meth)acrylate-based networks formed through photopolymerization possess material properties that can be easily tuned by control of chemistry and crosslinking density. The broad range of thermomechanical properties in these networks enables the development of various material platforms ranging from hydrogels [21,23] to biodegradable networks [23] to shape memory polymers [3,24]. However, the toughness of photopolymerized (meth)acrylate networks is limited for long term use in high loading environments, especially under aqueous conditions.

Therefore, the objective of this study is to understand the role of the glass transition behavior and water content on network toughness under physiological conditions. The approach involves performing stress–strain measurements in parallel with differential scanning calorimetry (DSC) and thermogravimetric analysis (TGA) on two model ternary (meth)acrylate networks, MMA-co-MA-co-PEGDMA and 2HEMA-co-BMA-co-PEGDMA. Different compositions of each network are formulated by varying the weight ratios of the two linear monomers (MMA:MA or BMA:2HEMA). The first aim is to identify how the T_g of each network changes as the composition changes in both air and PBS. Secondly, the swelling behavior as a function of composition is evaluated and related to the T_g of each network immersed in PBS. Finally, toughness is determined in air and PBS at 37 °C to identify relationships between chemistry and toughness. From this study, two materials with enhanced toughness are identified and it is shown that network toughening is achieved through different mechanisms in each network.

2. Materials and methods

2.1. Materials

Methyl methacrylate (MMA), methyl acrylate (MA), benzyl methacrylate (BMA) and 2-hydroxyethyl methacrylate (2HEMA) monomers, and poly(ethylene glycol) dimethacrylate (PEGDMA) crosslinker with a molecular weight of $M_n \sim 750$ were obtained from Sigma–Aldrich and used as-received. 2,2 Dimethoxy 2-phenylacetophenone (DMPA) was used as the photoinitiator and was purchased from Sigma–Aldrich as well. The chemical structures of monomers used are presented in Fig. 1.

2.2. Synthesis

Monomer solutions were formulated by combining two monofunctional acrylates or (meth)acrylates (MA and MMA or BMA and

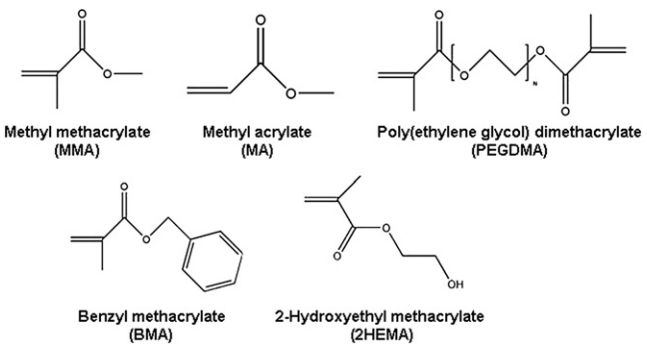

Fig. 1. Chemical structures of monomers incorporated into ternary networks.

Table 1
Formulated compositions of MA-co-MMA-co-PEGDMA consisting of 10wt.% PEGDMA ($M_n \sim 750$) and MA and MMA with weight ratios listed (by weight) of MA:MMA. The T_g's in air and PBS measured through DSC are listed as well as the swelling ratios (q) determined after immersion in PBS for 1 week.

Name	wt.% MA:MMA	T_g (°C)		q
		Air	PBS	
18%MA-co-MMA-co-PEGDMA	20:80	49.5 ± 0.5	48.9 ± 3.1	1.01 ± 0.010
27%MA-co-MMA-co-PEGDMA	30:70	46.3 ± 2.3	41.0 ± 0.8	1.03 ± 0.002
29%MA-co-MMA-co-PEGDMA	32:58	46.7 ± 2.8	41.4 ± 1.2	1.02 ± 0.005
31%MA-co-MMA-co-PEGDMA	34:56	45.6 ± 8.5	39.0 ± 0.2	1.03 ± 0.003
34%MA-co-MMA-co-PEGDMA	38:52	43.8 ± 2.2	34.3 ± 3.3	1.03 ± 0.008
36%MA-co-MMA-co-PEGDMA	40:60	43.8 ± 1.6	34.2 ± 3.1	1.03 ± 0.008
40%MA-co-MMA-co-PEGDMA	45:55	35.4 ± 3.0	18.5 ± 4.7	1.04 ± 0.010
54%MA-co-MMA-co-PEGDMA	60:40	28.1 ± 0.9	13.1 ± 2.4	1.03 ± 0.003
63%MA-co-MMA-co-PEGDMA	70:30	20.4 ± 0.7	9.3 ± 0.4	1.03 ± 0.004
72%MA-co-MMA-co-PEGDMA	80:20	21.5 ± 4.3	5.3 ± 2.8	1.04 ± 0.004

2HEMA) and a difunctional (meth)acrylate (PEGDMA). MA-co-MMA-co-PEGDMA solutions were prepared by combining ratios of MA and MMA determined by weight percentage with 10% PEGDMA and 1% DMPA. The weight percentages of MA and MMA used for each composition are listed in Table 1. 2HEMA-co-BMA-co-PEGDMA solutions were prepared by combining different ratios of BMA and 2HEMA determined by weight percentage with 2% PEGDMA and 0.5% DMPA. The weight percentages of BMA and 2HEMA used for each composition are listed in Table 2.

Each solution was mixed manually in a glass vial and injected between two glass slides using a glass pipette. Slides were separated with two 1 mm glass spacers. To prevent leakage of the MA-co-MMA-co-PEGDMA solution, all four sides of the slides were taped. Slides were coated with Rain-X to enhance release. Due to the strong adhesiveness of 2HEMA, slides used for the 2HEMA-co-BMA-co-PEGDMA solutions were coated with poly(dimethylsiloxane) (PDMS; Dow Corning Sylgard 184), instead of Rain-X, to prevent adhesion and to enhance release. The samples were placed in a UV chamber (Model CL-1000L Ultraviolet Crosslinker; $\lambda = 365$ nm; energy $= 2000 \times 100$ μJ/cm^2) for the minimal amount of time needed to fully polymerize (approximately 30 min and 10 min for MA-co-MMA-co-PEGDMA and 2HEMA-co-BMA-co-PEGDMA, respectively).

2.3. Differential scanning calorimetry

The glass transition temperature (T_g) of each network was determined by performing differential scanning calorimetry (DSC; TA Instruments Q100, Newcastle, DE) under a nitrogen environment. Samples were weighed on a balance (average sample mass between 10 and 15 mg) and then cooled to −80 °C and subsequently heated to 200 °C at a constant rate of 5 °C/min. T_g was denoted as the mid-point of the second order transition on the heating scan. Samples of each composition were soaked in phosphate buffered saline (PBS; Sigma Aldrich) for 1 week and run on the DSC using the same procedure. Before testing, each sample was removed from the solution and patted dry with a paper towel to remove excess moisture. Average T_g and standard deviation were calculated for each composition under each condition ($n = 3$).

2.4. Swelling study

To evaluate the equilibrium swelling behavior of each network, samples were soaked in PBS for 1 week. Each sample was laser-cut into a rectangular piece with a width of 5 mm and a length of 20 mm. Sample mass was measured after 1 week of soaking (W_W). Each sample was dried in a vacuum at 40 °C for 24 h and the mass was measured again (W_D). The swelling ratio (q) was calculated according to the formula:

$$q = W_w/W_D \quad (1)$$

Average q values and standard deviation were calculated for each composition ($n = 4$).

2.5. Thermogravimetric analysis

Mass loss as a function of temperature was determined using a thermogravimetric analyzer (TA instruments; New Castle, DE). Samples were tested under dry conditions and after soaking in PBS for 1 week. Those samples immersed in PBS were patted to remove excess surface moisture and then quickly loaded into the pan to avoid evaporation of PBS within the sample. Samples were heated from room temperature to 400 °C at a rate of 5 °C/min under a nitrogen environment. Sample mass (W_T) as a function of temperature was recorded for each sample, and total, free, and bound water contents were calculated according to previous studies [12,15,25]. Mean values and standard deviation of total water content and bound water content were calculated for each composition ($n = 3$).

2.6. Fourier transform infrared spectroscopy

Chemical structure for select networks was evaluated by performing Fourier transform infrared spectroscopy (FTIR) in total attenuated reflectance (ATR) mode using a Bruker Optics Tensor Spectrometer with a KBr crystal. Ten scans were obtained at 1 Hz on dry samples and samples immersed in PBS for one week. Prior to

Table 2
Formulated compositions of BMA-co-2HEMA-co-PEGDMA consisting of 2 wt.% PEGDMA ($M_n \sim 750$) and BMA and 2HEMA with weight ratios listed (by weight) of BMA:2HEMA. The T_g's in air and PBS measured through DSC are listed as well as the swelling ratios (q) determined after immersion in PBS for 1 week.

Name	wt.% 2HEMA:BMA	T_g (°C)		q
		Air	PBS	
98%BMA-co-PEGDMA	0:100	56.7 ± 1.6	52.8 ± 1.1	1.00 ± 0.001
19%2HEMA -co-BMA-co-PEGDMA	20:80	57.5 ± 1.3	50.4 ± 2.2	1.01 ± 0.002
39%2HEMA-co-BMA-co-PEGDMA	40:60	57.7 ± 2.7	41.7 ± 1.7	1.02 ± 0.002
49%2HEMA-co-BMA-co-PEGDMA	50:50	55.7 ± 0.9	41.9 ± 0.5	1.03 ± 0.004
54%2HEMA-co-BMA-co-PEGDMA	55:45	54.6 ± 1.8	38.8 ± 3.5	1.05 ± 0.008
59%2HEMA-co-BMA-co-PEGDMA	60:40	55.6 ± 1.0	35.7 ± 1.5	1.06 ± 0.008
64%2HEMA-co-BMA-co-PEGDMA	65:35	57.7 ± 0.9	33.8 ± 2.3	1.11 ± 0.006
69%2HEMA-co-BMA-co-PEGDMA	70:30	57.7 ± 0.3	28.9 ± 1.1	1.14 ± .006
73%2HEMA-co-BMA-co-PEGDMA	75:25	57.1 ± 0.5	21.8 ± 2.1	1.16 ± .007
78%2HEMA-co-BMA-co-PEGDMA	80:20	56.2 ± 0.8	18.9 ± 0.3	1.21 ± 0.007
98%2HEMA-co-PEGDMA	100:0	58.1 ± 0.3	19.8 ± 0.5	1.65 ± 0.030

obtaining spectra, wet samples were patted lightly to remove bulk water on the surface and then immediately placed on the crystal. Peak wavenumbers were identified using the OMNIC software. 3 samples were scanned per condition.

2.7. Tensile testing

Tensile strain-to-failure tests were performed on a universal testing machine (MTS Insight 2) using a 2kN load cell. Dogbone samples were laser-cut according to dimensions specified in ASTM D 638-03 Type IV with a 20 mm gauge length and a 2.8 mm gauge width. Before testing, the edges were sanded to remove any defects from the laser, and the width and thickness in the gauge section were measured using digital calipers. The samples tested in air were loaded in tensile grips, heated to 37 °C in a thermal chamber, and held at 37 °C for 10 min to allow for thermal equilibration. For testing under aqueous conditions, samples were soaked in PBS for 1 week. Prior to testing, the sample was removed from the PBS, patted with a paper towel to remove excess PBS, and its dimensions were measured using digital calipers. The soaked samples were loaded in tensile grips, submerged in a PBS bath at 37 °C, and held at 37 °C for 10 min to allow for thermal equilibration. All tests for these compositions were conducted at a strain rate of 5%/s. Only samples that broke in their gauge length were used for property calculations. Toughness was calculated as the area under the stress–strain curve in units of MJ/m^3. Elastic modulus was calculated as the slope of the initial linear portion of the stress strain curve for each test.

Based on the results of the initial tests, one composition each of MA-co-MMA-co-PEGDMA and 2HEMA-co-BMA-co-PEGDMA underwent further tensile testing in PBS using the same procedure, but at different strain rates of 0.05%/s, 0.5%/s, and 50%/s. Average toughness values and standard deviation were calculated for each composition. Compositions were tested four times at each strain rate under each condition (dry or wet).

3. Results

3.1. Differential scanning calorimetry

Representative DSC heat flow curves normalized by the sample mass are shown in Fig. 2 for various compositions of MA-co-MMA-co-PEGDMA and 2HEMA-co-BMA-co-PEGDMA networks under dry and aqueous conditions. T_g is denoted on a sample curve as the second order change in heat flow. Looking at the thermograms of 98%2HEMA-co-PEGDMA, peaks are observed at 0 °C and 100 °C corresponding to water in the network undergoing a phase change. PBS evaporation can be observed in the thermograms of other compositions as minima in the heating curve that occurs around 100 °C. In the 2HEMA-co-BMA-co-PEGDMA system, the area of these minima increases as more 2HEMA is added to the network. A similar minimum is observed in the MA-co-MMA-co-PEGDMA networks although there is no observable difference in area with changing composition.

Average T_g's measured from the DSC are listed in Tables 1 and 2 and graphed in Fig. 3 as a function of MA or 2HEMA percent weight fractions for MA-co-MMA-co-PEGDMA and 2HEMA-co-BMA-co-PEGDMA, respectively. For the MA-co-MMA-co-PEGDMA network, T_g decreases in both air and in PBS as the MA concentration increases with average values ranging from 49.47 °C to 21.47 °C and 48.90 °C to 5.2 °C, respectively. For each composition, the average T_g value in PBS is lower than the average T_g value in air. By comparing the change in T_g with composition, the T_g of 29%MA-co-MMA-co-PEGDMA decreases by 5 °C; whereas, 72%MA-co-MMA-co-PEGDMA experiences a 15 °C reduction in T_g when immersed in PBS. Similarly, T_g linearly depends on the weight fraction of MA under both dry and wet conditions, but this linear relationship between T_g and MA concentration in PBS has a larger slope compared with dry conditions indicating that T_g is decreased to a greater extent in PBS as more MA is added to the network. Similarly, increasing the 2HEMA concentration in the 2HEMA-co-BMA-co-PEGDMA networks results in an incremental decrease in T_g in PBS with values ranging from 52.84 °C to 19.79 °C, but under dry conditions, the T_g is independent of relative BMA and 2HEMA concentrations. The decrease in T_g with PBS exhibits a nonlinear behavior converse to the relationship in MA-co-MMA-co-PEGDMA.

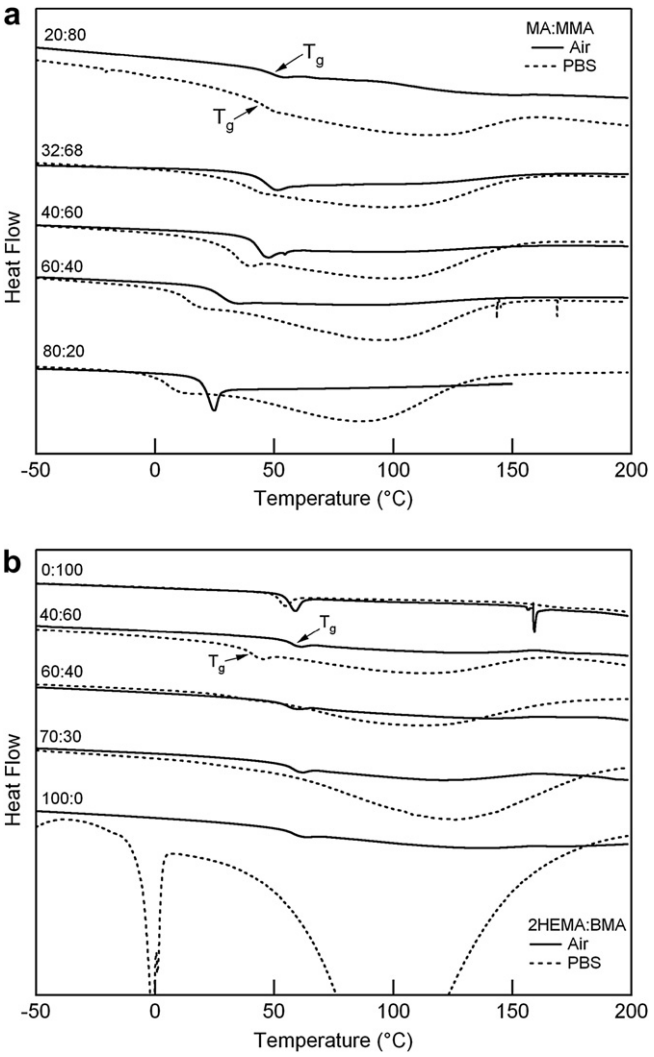

Fig. 2. Representative DSC scans of (a) MA-co-MMA-co-PEGDMA and (b) BMA-co-2HEMA-co-PEGDMA for select compositions (MA:MMA) under dry (solid line) and wet (dashed line) conditions. T_g as defined in the methods is indicated for one sample composition.

Although these measured T_g values might be considered low, especially for the 98%2HEMA-co-PEGDMA material, it has been previously shown that T_g will vary depending on the analysis technique adopted (i.e. DSC vs. dynamic mechanical analysis) [26]. In this study, DMA was initially performed on all compositions with T_g defined as the temperature where the tan delta reaches a maximum. It was determined that the T_g measured by DSC coincided with the onset temperature of the thermomechanical glass transition observed on the DMA (data not shown). Due to this

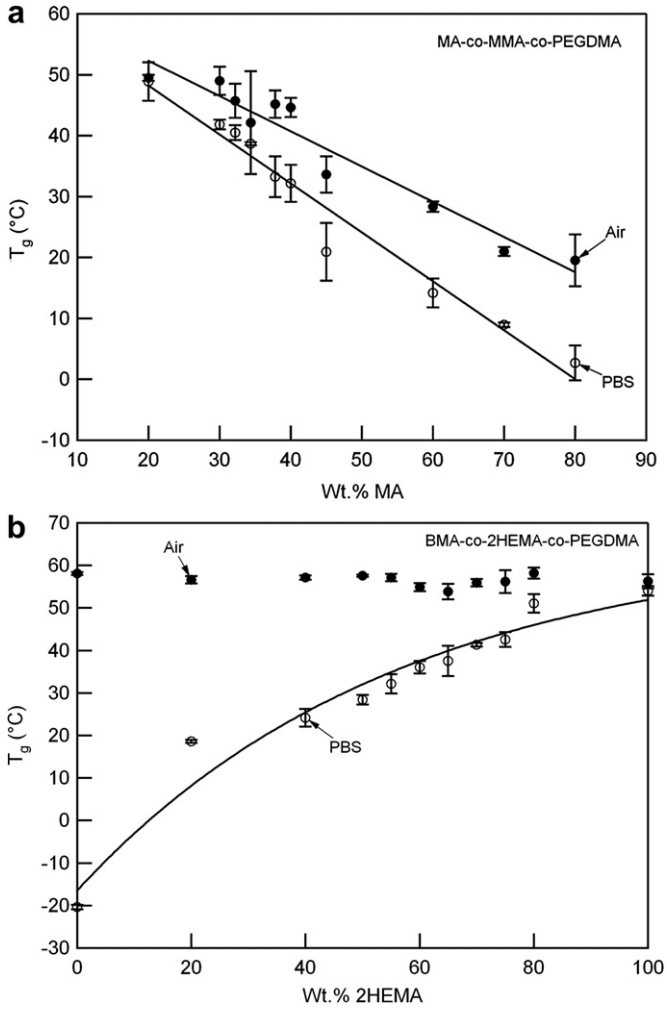

Fig. 3. Effect of varying the MA concentration on T_g under both dry and wet conditions for a) MA-co-MMA-co-PEGDMA and b) BMA-co-2HEMA-co-PEGDMA. Average values are presented with standard deviation for each composition. A curve was fit to the experimental data under each condition and is included.

difference, the T_g's determined by DSC will be coincidentally lower than expected to an extent determined by the breadth of the network's glass transition behavior [26].

3.2. Equilibrium swelling behavior

Average swelling ratios (q) for each composition of MA-co-MMA-co-PEGDMA and 2HEMA-co-BMA-co-PEGDMA are displayed in Tables 1 and 2, respectively. T_g as a function of water absorption is shown for the two networks in Fig. 4. In the MA-co-MMA-co-PEGDMA network, changing the MA concentration has no effect on water absorption with all networks exhibiting similar swelling ratios ($q \approx 1.03$–1.04). Conversely, water content in 2HEMA-co-BMA-co-PEGDMA increases as the concentration of 2HEMA increases with the swelling ratio reaching a maximum of 1.65 in the 98%2HEMA-co-PEGDMA network.

3.3. Thermogravimetric analysis

The total water content and fraction of bound water in select compositions of each network were determined through TGA.

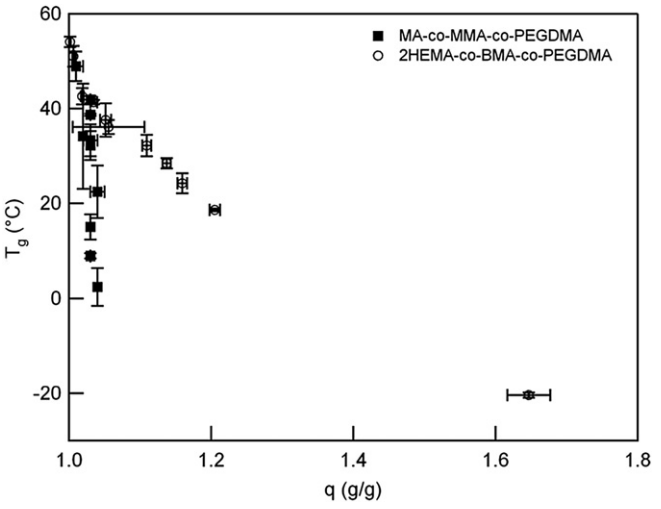

Fig. 4. Effect of water absorption (as measured by the swelling ratio "q") on the T_g of each network. Average values +/− standard deviation are presented for each composition.

Representative DT/TGA plots of 29%MA-co-MMA-co-PEGDMA and 59%2HEMA-co-BMA-co-PEGDMA are shown in Fig. 5. Sample mass (M_T) at each temperature point was used to calculate the percent of the initial sample mass remaining ($\%M_o$) by:

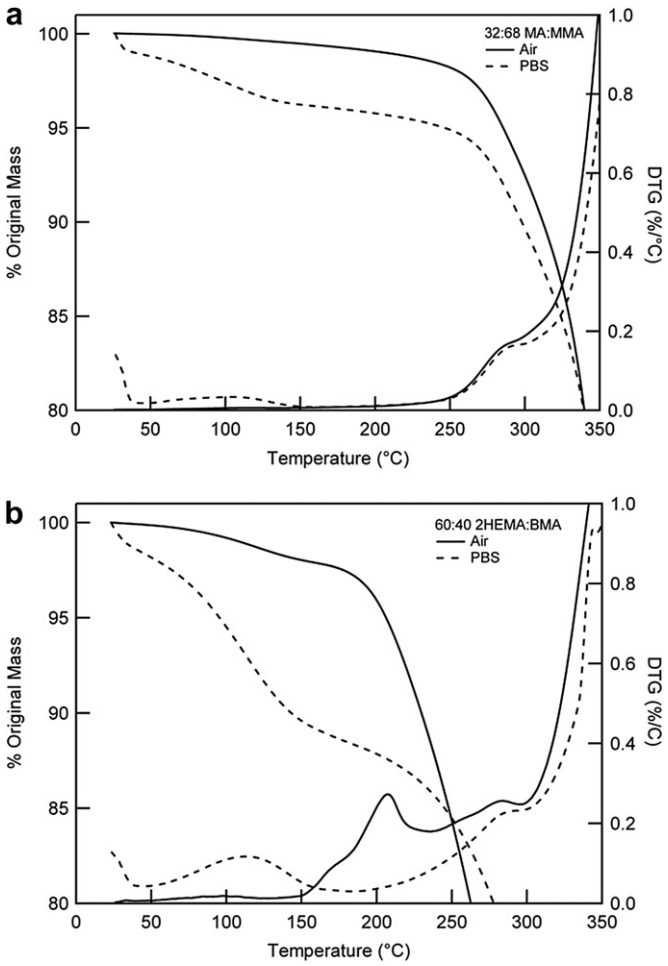

Fig. 5. Representative TGA results of (a) 29%MA-co-MMA-co-PEGDMA (32:68) and (b) 59%2HEMA-co-BMA-co-PEGDMA (60:40) in air and after 1 week immersion in PBS.

$$\%M_o = \frac{M_T}{M_o} \times 100 \quad (2)$$

where M_o is the initial sample mass (10–15 mg). $\%M_o$ was plotted as a function of temperature along with the derivative change in weight with temperature (DTG). Initial decomposition temperature was defined as the temperature where the DTG began to increase rapidly above 100 °C. TGA profiles of other tested compositions were not included for clarity purposes, but exhibited similar behavior in comparison to the mass loss of dry and soaked samples. The presence of free water can be observed by the decrease in mass and rapid increase in DTG below 100 °C compared with the thermograms for dry samples. Above 100 °C, a greater mass loss also occurs in the PBS-soaked samples due to bound water eventually evaporating at a higher temperature. In the 32:68 MA network, this maxima is very broad and shallow; whereas, the 60:40 2HEMA network exhibits a higher and broader maxima in DTG with the rate peaking around 120 °C. The effect of PBS on the thermal stability of the 2HEMA network is also evident by the increased decomposition temperature compared with dry samples.

Following the methods of previous studies [12,18], the total water content (W_t) was defined as:

$$W_t = 100 - \%M_D \quad (3)$$

where the $\%M_D$ is defined as the percent sample weight at a temperature slightly below the decomposition temperature for the network. Because BMA decomposes at a low temperature (around 180 °C), this was the temperature commonly adopted for the different compositions of BMA-co-2HEMA-co-PEGDMA network while the initial decomposition temperatures for various formulations of MA-co-MMA-co-PEGDMA ranged from 180 °C to 200 °C. The amount of free water was defined as:

$$W_f = 100 - \%M_T \quad (4)$$

where $\%M_T$ is the percent sample mass at 100 °C. Although it would be expected that PBS would evaporate at a higher temperature compared with pure water, thermograms from TGA performed on bulk PBS showed complete evaporation of the water by 100 °C. suggesting that the salt content, in this case, did not affect the overall phase transitions of the solution. Thus, it was assumed that PBS not directly hydrogen bonded with the network (the termed, "free water") will evaporate in a manner similar to its bulk state at 100 °C. This temperature was adopted to determine the weight fraction of free water. Because bound water is in phase with the polymer network, these molecules will boil at a much higher temperature, oftentimes when the polymer begins to decompose. By assuming water can only be found in one of two states, the difference between the total water content and free water content was defined as the bound water within the network [18]. The total water and bound water content calculated from these plots for all compositions are shown in Fig. 6. To determine if water state changes in the network independently of changes in total water content, the ratio of bound water to total water content are included for comparison.

Consistent with swelling measurements, average total water content and bound water content (3.5–5.2% and 0.8–2.0%, respectively) remain relatively constant in the MA-co-MMA-co-PEGDMA network despite changing the MA concentration. The total water contents measured from TGA were consistent with the swelling ratios for the different compositions of MA-co-MMA-co-PEGDMA network. Interestingly, the ratio of bound water to total water content is higher for networks containing more MMA vs. MA indicating that water behavior is dependent on the copolymer

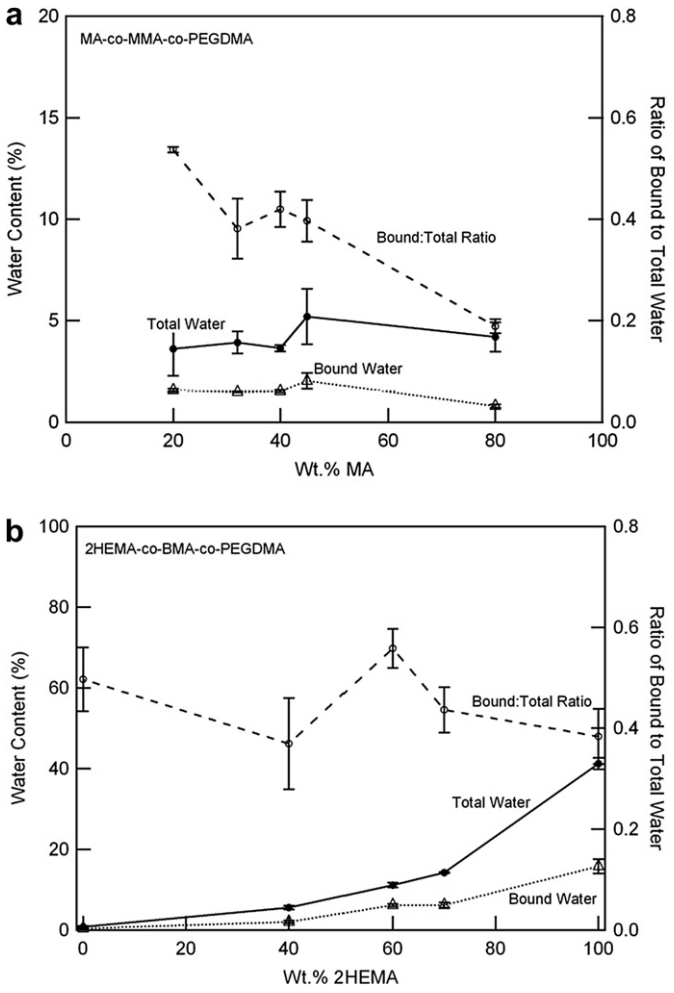

Fig. 6. Average values of total and bound water content as a function of (a) MA concentration or (b) 2HEMA concentration. The ratio of the bound to total water content is shown and represents average values +/− standard deviation calculated for several different compositions ($n = 3$).

composition. In the 2HEMA-co-BMA-co-PEGDMA network, both total water content and bound water content (1% to 41.2% and less than 1%–15.8%, respectively) increase as the concentration of 2HEMA increases, but there is no significant change in the ratio of bound to total water content. For formulations of the 2HEMA-co-BMA-co-PEGDMA networks containing more than 60% 2HEMA, the water contents as measured through TGA were lower compared to the fraction of absorbed water extracted from the calculated swelling ratio. It is possible that some PBS evaporated during loading the sample into the TGA resulting in less mass loss due to water evaporation during heating. This effect was mitigated as best as possible by keeping samples hydrated prior to testing and quickly loading the samples before testing. It is also important to recognize that the two states of water described above are the extremes in a continuum of water states that exist within a polymer. More extensive studies of the thermal transitions of water in polymers have been detailed elsewhere and were beyond the scope of this study [19,27,28].

3.4. Fourier transform infrared spectroscopy

To better understand the water–polymer interactions in the MA-co-MMA-co-PEGDMA network, FTIR-ATR was performed on

select compositions. Representative FTIR spectra of 29%MA-co-MMA-co-PEGDMA, 40%MA-co-MMA-co-PEGDMA, and 63%MA-co-MMA-co-PEGDMA under both dry and wet conditions are shown in Fig. 7. The peaks at 1160 cm^{-1}, 1730 cm^{-1}, and 2950 cm^{-1} correspond to the C–O–C stretching vibrations, C═O stretching vibration, and C–H stretching vibrations (for the methyl groups), respectively. A slight change in intensity in the C–O–C and C═O vibrational bands under wet conditions is observed, particularly in the 45:55 and 32:68 compositions, due to the formation of hydrogen bonds with surrounding water molecules (Fig. 7a). After immersion in PBS, peaks appear around 1650–1700 cm^{-1} and 3400–3600 cm^{-1} corresponding to O–H bending and stretching vibrations of the water molecules, respectively. The shifts in the O–H stretching and O–H bending bands to higher frequencies are indicative of the hydrophobicity of the network due to less hydrogen bond formations between adjacent water molecules and/or water molecules with polymer chains [29]. Comparing the frequencies amongst the three compositions in Fig. 7b, a right shift in the peak frequency for O–H stretching occurs in the 32:68 formulation compared to the other two compositions suggesting that hydrogen bonding is stronger in networks with lower MA concentration.

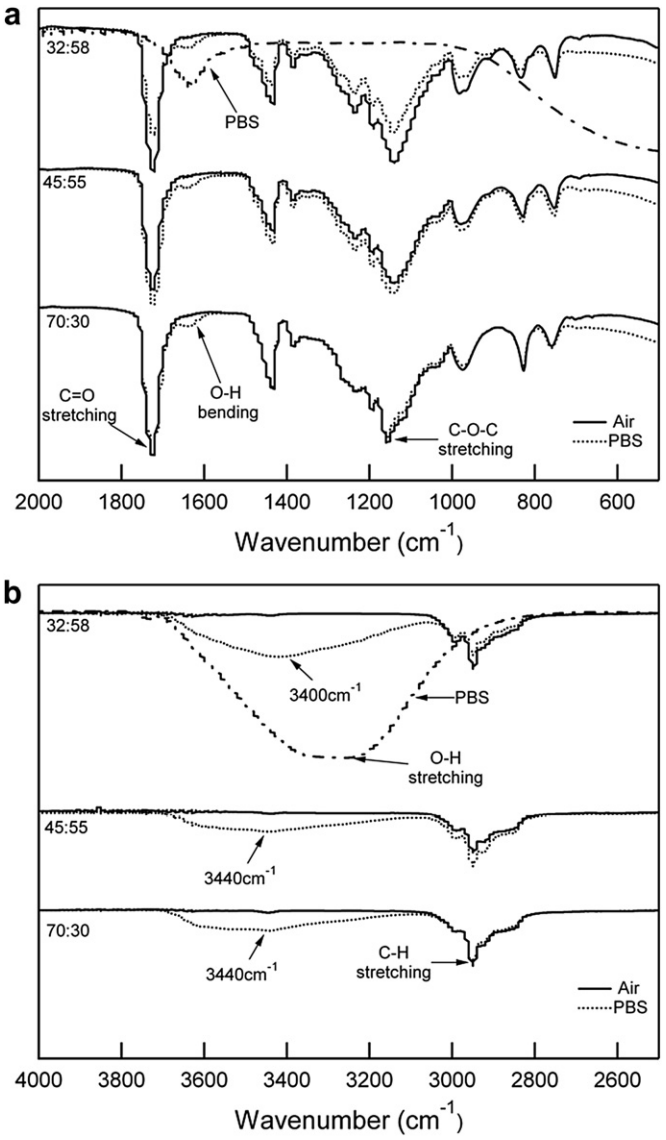

Fig. 7. Representative FTIR-ATR spectra in the (a) low frequency range and (b) high frequency range for select MA-co-MMA-co-PEGDMA compositions (MA:MMA) under dry conditions and after 1 week immersion in PBS.

3.5. Stress–strain behavior

Representative stress–strain behaviors of MA-co-MMA-co-PEGDMA and 2HEMA-co-BMA-co-PEGDMA at different compositions under both dry and wet conditions at 37 °C are shown in Figs. 8 and 9, respectively. For each composition, the stress–strain behavior is altered in PBS exhibiting a decreased modulus, reduced strength and increased failure strain compared to dry conditions. Under both dry and wet conditions, the MA-co-MMA-co-PEGDMA network exhibits a transition from brittle to ductile to rubbery behavior as MA concentration is systematically increased as indicated by a gradual decrease in modulus, the appearance and waning of yielding behavior, and increase in failure strain. Comparing Fig. 8a and b, the stress–strain behavior at each composition in air does not match the behavior of that same composition when soaked in PBS, but instead exhibits more ductile (i.e. 30:70) or rubbery (i.e. 45:55) mechanical behavior. In air, the stress–strain behavior of 2HEMA-co-BMA-co-PEGDMA was not affected by changing the 2HEMA concentration, but maintained brittle behavior independent of composition (data not shown). In PBS, 2HEMA-co-BMA-co-PEGDMA showed a similar relationship between composition and stress strain behavior as

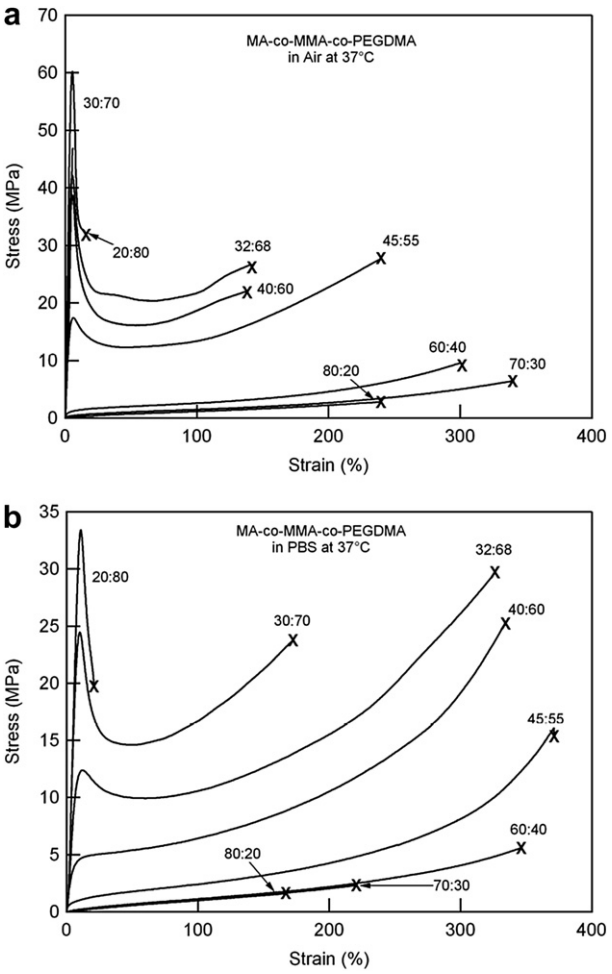

Fig. 8. Stress–strain behavior of MA-co-MMA-co-PEGDMA at different ratios of MA:MMA tested in (a) air and (b) PBS at 37 °C.

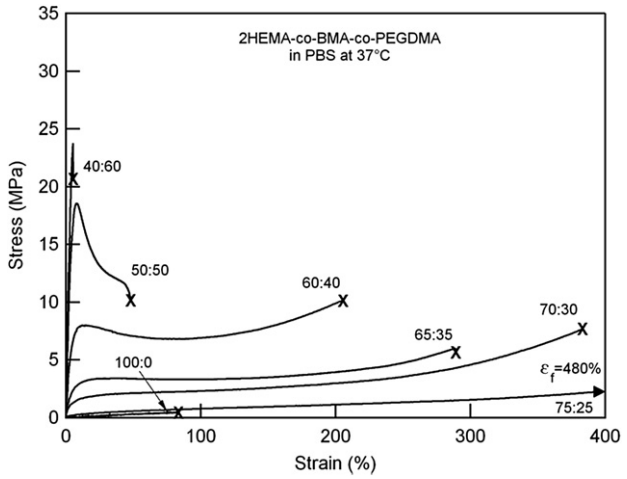

Fig. 9. Stress–strain behavior of 2HEMA-co-BMA-co-PEGDMA at different ratios of 2HEMA:BMA tested in PBS at 37 °C.

MA-co-MMA-co-PEGDMA with a glassy to rubbery transition occurring with increasing 2HEMA content.

3.6. Effect of composition on toughness

Using the area under the stress–strain curves, toughness is plotted as a function of MA or 2HEMA concentration as shown in Fig. 10. In the MA-co-MMA-co-PEGDMA network, a peak in toughness in air and PBS occurs at the composition with 32%MA while an additional peak is also observed in air at the 45%MA composition. These peak compositions are easily identified as their toughness values are several orders of magnitude higher compared with other MA concentrations within the network. In comparison to MA-co-MMA-co-PEGDMA, the toughness of 2HEMA-co-BMA-co-PEGDMA in air is low and does not vary with changing 2HEMA concentration. In PBS, toughness is the highest for 59%2HEMA-co-BMA-co-PEGDMA and then decreases with increasing or decreasing 2HEMA concentration.

3.7. Effect of strain rate on toughness

The effect of strain rate on the toughness of 59%2HEMA-co-BMA-co-PEGDMA and 29%MA-co-MMA-co-PEGDMA is displayed in Fig. 11. In both networks, toughness is altered when the strain rate changes over several orders of magnitude. At 5%/s, the toughness of both MA-co-MMA-co-PEGDMA and 2HEMA-co-BMA-co-PEGDMA is highest (Fig. 8). As the strain rate decreases from 5%/s to 0.5%/s to 0.05%/s, network toughness gradually decreases with the MA-co-MMA-co-PEGDMA network exhibiting the larger change in toughness compared with 2HEMA-co-BMA-co-PEGDMA networks. The toughness of 59%2HEMA-co-BMA-co-PEGDMA does not change when tested between rates of 0.5–50%/s but declines slightly when tested at 0.05%/s.

4. Discussion

Increased moisture content as a result of implantation into hydrated areas of the body is a common cause of mechanical failure for polymeric biomaterials. In many instances, it is necessary that the material be able to absorb a large amount of water (for example, in hydrogels) to serve its desired function in the body as well as maintain suitable mechanical properties to ensure durability and long term functionality. A polymer

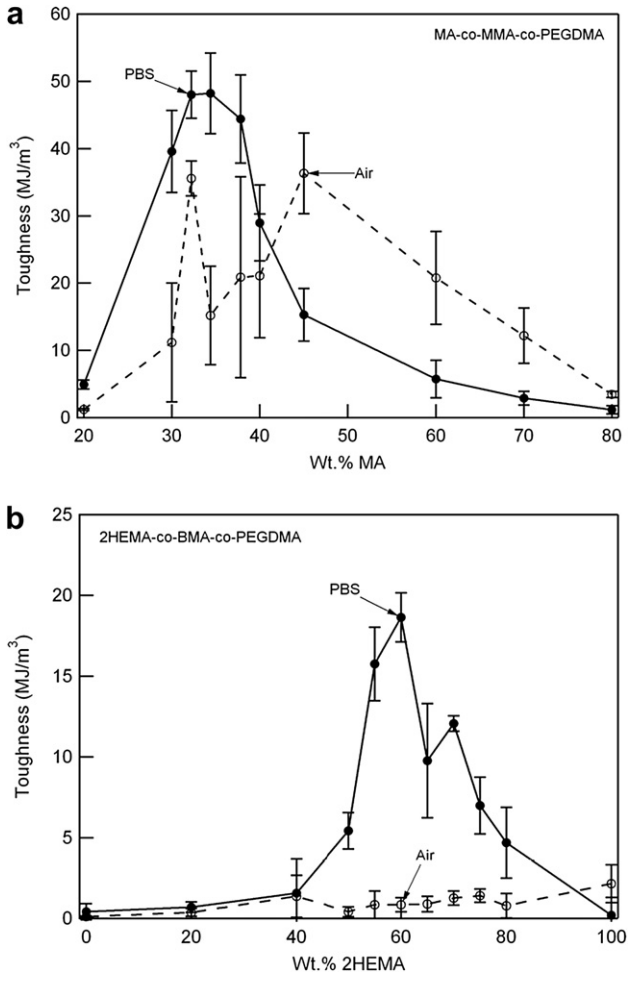

Fig. 10. Toughness plotted as a function of composition for (a) MA-co-MMA-co-PEGDMA and (b) BMA-co-2HEMA-co-PEGDMA. The toughness under both dry (dotted line) and wet (solid line) are compared for each network.

biomaterial that is tough in solution would serve a variety of applications including a shape memory fixation device, compliant soft tissue replacement, hydrogel and/or tissue engineering scaffold. Although the materials studied here are non-degradable,

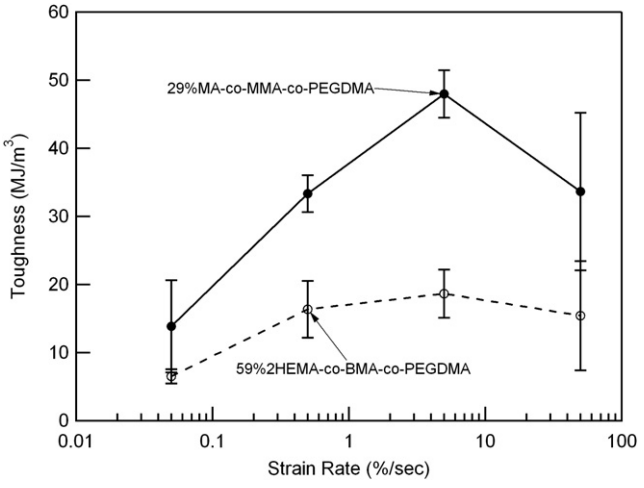

Fig. 11. The effect of strain rate on the toughness of 29%MA-co-MMA-co-PEGDMA and 59%2HEMA-co-BMA-co-PEGDMA networks tested in PBS at 37 °C.

the concepts discussed herein may be extended to certain degradable polymer networks.

In this study, the influence of an aqueous environment on the toughness of photopolymerizable (meth)acrylate networks was examined using two ternary copolymer networks. Three component networks allow for the systematic control of various materials properties, such as T_g, by varying the weight ratio of the two linear monomers without changing the crosslinker concentration. Maintaining a constant crosslinker concentration is important as it has been shown that crosslinking density will affect water absorption and the mechanical properties independent of monomer chemistry. The combinations of linear monomers incorporated into each network were chosen for several reasons. In one network, MA and MMA were selected because they have different T_g's (−10 °C and 130 °C, respectively), but their structures provide a similar level of hydrophobicity based on polarity (Fig. 1). Previous studies also revealed that MA-co-MMA-co-PEGDMA (with 2% PEGDMA) has inherently high toughness with an elastic modulus in the range of many tough biological tissues [7]. Conversely, the two linear monomers selected for the second network, BMA and 2HEMA, both have high T_g's in relation to body temperature (80 °C and 110 °C, respectively), but have side groups with opposing degrees of hydrophilicity (Fig. 1). In addition, 2HEMA is a monomer that is extensively used in contact lenses and hydrogels [30,31] while BMA has been shown to have enhanced toughness at its glass transition temperature [32]. From the results presented here, it can be suggested that network toughness under physiological conditions is dependent on T_g, water absorption, and strain rate, in a manner related to network composition. In the following discussion, the individual role of each property on enhancing toughness, with respect to each network, will be examined as well as how these properties are interrelated in affecting toughness.

In the MA-co-MMA-co-PEGDMA system, T_g is dependent on MA concentration under both dry and wet conditions. The observed decrease in T_g with increasing MA concentration (Fig. 3) can be explained by considering that the T_g of a copolymer network is dependent on the individual T_g's and concentrations of the monomer components [33,34]. Because MA has a lower T_g compared to MMA and the PEGDMA concentration is constant in all network formulations, the T_g of the MA-co-MMA-co-PEGDMA network effectively decreases as more MA is added to the network. After immersion in PBS for 1 week, the T_g of each composition in PBS decreases indicating that water molecules are being absorbed and changing the thermodynamic state of the network. Due to the low water content in the network, the absorbed water molecules are effectively acting as a plasticizer by increasing the configurational entropy accessible to the network in a manner related by the following expression derived from the Couchman equation:

$$\Delta S^c = -C_p \ln\left(\frac{T_{gPBS}}{T_{gAir}}\right) \tag{5}$$

where ΔS^c is the change in the configurational entropy of mixing and C_p is the heat capacity of the network [33]. If it is assumed that heat capacity is not affected by the plasticizer, the larger increase in T_g with networks with higher MA concentration suggests that ΔS^c due to the introduction of PBS is composition-dependent. Several theories have been developed to predict the effect of water and copolymer composition on T_g including the Gordon–Taylor [35] and Couchman-Karaz equations [33,36]. Because the total water content of MA-co-MMA-co-PEGDMA is low, it is difficult to apply these equations in predicting T_g as the concentration of the liquid diluent, PBS, is small enough such that it is difficult to ascertain if the diluent T_g would remain the same as in the bulk. The linear relationship between T_g and MA concentration suggests that this copolymer network follows simple additive properties related to the ideal volume of mixing, even in the presence of PBS [33,34]. However, it is also important to note that these theories are simplistic in that they only take into account two-component systems and thus cannot be fully utilized to account for change in both the copolymer concentration and changes in water content.

Besides considering the change in thermodynamics associated with mixing the PBS and polymer chains, it is important to consider how the specific water state is changing within the different compositions. It has previously been reported that the state of water molecules within the polymer can directly attribute to its glass transition behavior [12,28]. Considering that water content of the network is not affected by MA concentration (Fig. 4), the larger T_g reduction with increasing MA concentration in PBS (Fig. 3) suggests that the weight ratio of MA to MMA in the network could be affecting the state of the sorbed water molecules resulting in differential decreases in T_g [12,37]. Due to the difficulty in discerning the relative bound and free water contents, several different experimental techniques including DSC, TGA, and FTIR are usually employed to determine specific water–polymer interactions [12,14,27,29,38]. Because all MA-co-MMA-co-PEGDMA formulations have low water contents, the free water and bound water contents were undetectable through DSC. By considering that bound water will evaporate at a higher temperature due to its formation of a one-phase system with the network in comparison with free water which evaporates at 100 °C similar to bulk water, the free and bound water fractions can be determined through thermogravimetric analysis [12,25]. The observed 1–2% weight fraction of bound water, independent of MA concentration, (Fig. 6a) compares with other reported findings on polyurethanes that possess similar chemistry and hydrophobicity [12].

It might be expected that polymer networks with very low water content would not contain any unbound or free water, but rather all sorbed molecules would bind to any available hydrophilic chemical groups. However, the absence of potential binding sites in hydrophobic networks such as MA-co-MMA-co-PEGDMA causes sorbed water molecules to remain in an unbound state and arrange themselves into clusters in order to optimize the number of hydrogen bond interactions as well as minimize their interaction with the less energetically favorable hydrophobic components of the network [39]. These clusters will be located within the micropores of the network and exhibit a phase transition behavior characteristic of bulk water [28,29,40,41]. Although MA-co-MMA-co-PEGDMA is mostly hydrophobic, it is also evident from the FTIR spectra (Fig. 7) that some water is still present in a bound state, forming hydrogen bonds with ethylene glycol on PEGDMA and the ester groups located in the acrylate subunits.

Interestingly by comparing the ratio of bound water to total water content in the network, it is observed that the bound water content relative to total water content decreases with increasing MA concentration suggesting that water prefers to remain in an unbound state as MA concentration increases (Fig. 6). The lower O–H stretching frequency in the FTIR spectra of 29%MA-co-MMA-co-PEGDMA compared with the 63%MA and 40%MA formulations provides further evidence that more hydrogen bonding is occurring in formulations with less MA incorporated (Fig. 7b). Taking into consideration that free water content increases and T_g decreases to a greater extent with MA concentration (Fig. 2), it can be suggested that the extent of T_g reduction in PBS is dependent upon the free water content within the network. To follow up on this theory, DSC was performed using a heat-cool-heat scanning procedure on select MA-MMA compositions after 1 week immersion in PBS (data not shown). Samples were heated to a certain temperature, T_1 = 100 °C, 120 °C, or 140 °C, then cooled to 0 °C, held isothermal for 5 min, and reheated once again to 200 °C. An increase in T_g after

heating to only 100 °C indicates that the removal of free water is causing the T_g of the network to return to its original state for the dry network. Although T_g was further increased upon heating to higher temperatures, the greatest increase in T_g occurred in the heating scans ramping to 100 °C providing further evidence that the effect of PBS immersion on the T_g of MA-co-MMA-co-PEGDMA is governed by the presence of free water in the network.

By comparing the results in Figs. 3, 4, and 6, it is evident that the T_g of 2HEMA-co-BMA-co-PEGDMA is affected by PBS in a different manner compared with MA-co-MMA-co-PEGDMA. Unlike MA-co-MMA-co-PEGDMA, the 2HEMA concentration of 2HEMA-co-BMA-co-PEGDMA does not impact the T_g of the network under dry conditions (Fig. 3b). Because BMA and 2HEMA have similar reported T_g's [32,42], the T_g of the copolymer network will not be affected by changing the concentration ratio of 2HEMA to BMA, according to theories on the effect of copolymer mixing on T_g.[33–35] However after 1 week immersion in PBS, T_g becomes strongly dependent on 2HEMA concentration, an effect driven by the increased water content with increasing 2HEMA concentration (Figs. 3 and 4). In compositions with low water contents and little swellability (less than 60%2HEMA), the PBS is acting as a plasticizer, similar to the MA-co-MMA-co-PEGDMA network, to lower T_g by increasing the configurational entropy accessible to the network [33]. In this regime, the T_g experiences a few degrees reduction with an increase in 2HEMA (Table 1). In compositions containing more than 60%2HEMA, the 2-fold increase in network swellability (Table 1) indicates the polymer chains are being extended allowing for more PBS absorption, but less configurational entropy available to the network. In addition, the increased free volume allows the water molecules to act in a more stable state by forming hydrogen bonds with either the polymer chains or each other. The combination of these two mechanisms results in the T_g's of these compositions to decrease to a greater extent compared with the low 2HEMA compositions effectively leaving the networks in a relaxed, rubbery state.

When examining water state within the network, bound water content increases as more 2HEMA is added to the network as would be expected as more potential sites become available for water binding to occur (Fig. 6). Considering the polarity of the side groups of each monomer, it would be expected that the hydroxyl group in 2HEMA would readily form hydrogen bonds with adjacent water molecules. On the other hand, BMA contains a bulky, nonpolar phenyl ring in its side chain that limits the diffusion of water molecules and provides an energetically unfavorable environment for hydrogen bond formation to any hydrophilic components [14]. Unlike MA-co-MMA-co-PEGDMA, despite the change in water content with 2HEMA concentration, no trend is identified with the ratio of bound water to total water content indicating that the change in bound water with copolymer composition mirrors the change in total water content. This result in combination with the relationship between water state and T_g established in the MA-co-MMA-co-PEGDMA suggests that the individual influences of bound vs. free water on T_g depend on the total amount of water absorption into the network. However, further evidence would be needed to verify this theory and is beyond the scope of this study.

Considering these relationships between T_g and network chemistry, trends between toughness and T_g under both dry and wet conditions are identified in both networks. For MA-co-MMA-co-PEGDMA in air, toughness is affected by varying the MA concentration, reaching a maximum in 29%MA-co-MMA-co-PEGDMA and 40%MA-co-MMA-co-PEGDMA. By comparing the stress strain behavior in air and after immersion in PBS (Fig. 8), it is evident that the mechanical behavior of MA-co-MMA-co-PEGDMA is influenced by the presence of PBS in a manner that is dependent on network composition. Since the T_g of each composition is reduced when the network is immersed in PBS, the stress strain behavior is transitioning in a manner similar to increasing temperature. Similar to dry conditions, toughness in PBS varies with composition with a peak in toughness occurring in 29%MA-co-MMA-co-PEGDMA. Interestingly, this composition also exhibited enhanced toughness in air despite having a T_g well above testing temperature (47 °C). Looking at its stress strain behavior in Fig. 8, 29%MA-co-MMA-co-PEGDMA (32:68) exhibits higher failure strains and ultimate stresses compared to compositions with slightly more or less MA (i.e. 30:70 and 40:60 compositions). This unique behavior would enable the use of this material for an application where excellent mechanical properties were required under varying degrees of hydration.

In 2HEMA-co-BMA-co-PEGDMA, toughness in air is not affected by 2HEMA concentration, but rather remains low in all compositions. Because the T_g of this network is more than 25 °C above testing temperature, the material is acting in its glassy, brittle state. Like MA-co-MMA-co-PEGDMA, toughness of 2HEMA-co-BMA-co-PEGDMA is affected by immersion in PBS in a manner related to the concentration of 2HEMA incorporated into the network. Interestingly, toughness is enhanced in all formulations of the network indicating that water absorption can indeed act as a toughening mechanism in polymer networks under appropriate conditions. The toughness as a function of 2HEMA concentration displays a profile similar to the relationship between toughness and composition in MA-co-MMA-co-PEGDMA with toughness peaking in 59%2HEMA-co-BMA-co-PEGDMA (Fig. 10a vs. b). This composition exhibits slight yielding behavior, large failure strains (>200%) and some strain-induced hardening around 150% strain that all explain its enhanced toughness. When the BMA concentration reaches a certain amount (greater than 60%), both T_g and the stress strain behavior are affected little by immersion in PBS (Figs. 4 and 9). Despite having several hydrophilic components in the network, the bulkiness of BMA prevents few water molecules from binding and absorbing into the network as noted by the low water content present in these networks (Table 2 and Fig. 6).

Comparing the calculated toughness values between the two "peak" compositions, the average toughness is higher in 29%MA-co-MMA-co-PEGDMA network vs. 59%2HEMA-co-BMA-co-PEGDMA by more than 20 MJ/m^3. Because toughness is dependent on the magnitude of other mechanical properties including elastic modulus, failure strain, and ultimate strength, potential toughening mechanisms can be identified by examining the stress strain behavior. For example, 29%MA-co-MMA-co-PEGDMA possesses higher ultimate stresses and failure strains compared with 59%2HEMA-BMA-co-PEGDMA and also exhibits a strain-induced hardening effect (Fig. 8b vs. Fig. 9). The increased modulus and strength could be the result of the MA-co-MMA-co-PEGDMA network having a higher crosslinking concentration compared with 2HEMA-co-BMA-PEGDMA [3]. It has previously been proposed that strain hardening is induced by strong secondary bonding between the polymer chains [1] which will act to prevent chain displacement over larger ranges of loading. Although the formation of hydrogen bonds are unlikely between MA and MMA, hydrophobic bonding [43] between the side chains on the two monomers will enhance the strength of the polymer chains, an effect that would not be inhibited, but actually enhanced by the presence of water or PBS [14]. Since BMA and 2HEMA possess opposite polarities on their side chains, the secondary intermolecular bonding is weak within this network and even further weakened in solution, causing chains to be easily misaligned especially at higher strains.

Previous studies have proposed that toughness in acrylate-based networks will reach a peak at a certain temperature, and that when immersed in PBS, this toughness maximum in the same network will shift to a lower temperature [7]. Considering

this relationship between testing temperature and toughness in PBS, it can be suggested that optimal toughness occurs in PBS in the network whose T_g is reduced by PBS absorption in a manner that better aligns the temperature of optimal toughness with the testing temperature. For both the MA-co-MMA-co-PEGDMA and 2HEMA-co-BMA-co-PEGDMA networks, the compositions that possessed maximal toughness within each network (29%MA and 59%2HEMA, respectively) did in fact exhibit a T_g in PBS that was close to 37 °C (Tables 1 and 2 and Fig. 12). Therefore, a possible approach to attaining enhanced toughness under physiological conditions is creating a network whose T_g in PBS aligns with body temperature.

It is also important to note that enhanced toughness is only achieved within a certain range of moduli (5–600 MPa) for both networks (Fig. 13). This three order of magnitude range indicates the limits in regards to network stiffness available in designing a tough polymer biomaterial using a shift in T_g approach. Because a compliance mismatch between the biomaterial and surrounding tissue could warrant possible device failure and further injury, it is important to align the modulus of the polymeric biomaterial with the native tissue. Considering the possible load-bearing types of biological tissues for which photopolymerizable networks could be utilized towards (i.e. tendon $E = 100$–600 MPa; intervertebral disc $E = 1$–10 MPa), several compositions from each network with enhanced toughness could be selected that possess similar moduli to native tissue.

It is well understood that temperature and time effects on the deformation of polymers can be superimposed [42]. In this study, the two compositions for each network identified as having maximal toughness (29%MA-co-MMA-co-PEGDMA and 59%2HEMA-co-BMA-co-PEGDMA) were deformed under tension in PBS at various strain rates to determine the sensitivity of toughness to varying the time scale. In both networks, toughness changes when the strain rate changes over several orders of magnitude with a maximum in toughness occurring at 5% strain/s. This maximum is similar to the peak shown to occur in relation to the T_g of the network (Fig. 10), but occurs more broadly over the range of strain rates tested. In addition, changing the strain rate affects the toughness more in MA-co-MMA-co-PEGDMA compared with 2HEMA-co-BMA-co-PEGDMA. The acute glass transition behavior of this network as observed through dynamic mechanical analysis suggests that the mechanical behavior would be highly dependent on strain rate while the broad transition of BMA-co-2HEMA-co-PEGDMA networks makes this copolymer

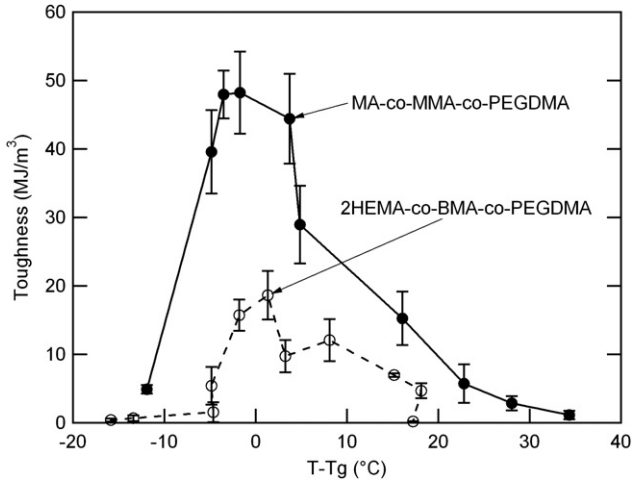

Fig. 12. Network toughness as a function of the temperature difference between the testing temperature (T), 37 °C in this case, and the T_g in PBS of that composition.

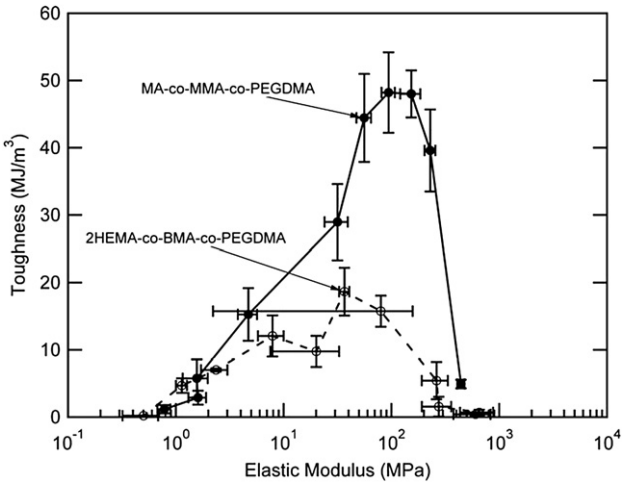

Fig. 13. Network toughness as a function of elastic modulus for both meth(acrylate) networks tested in PBS. Values in figure are averages of several tests run for each composition ($n = 4$).

less affected by the magnitudes of relevant time scales. From these results, it is important to consider the loading rate of the mechanical environment to which the (meth)acrylate network would be utilized in the body. For the purposes of this study, the rates chosen represent loading rates that occur in the knee or spine under resting, normal, and high levels of activity [44].

Because the intended use of these networks is in an implantable biomaterial, PBS as a solvent was chosen to better mimic the physiological fluid and pH of the body. Although it is possible that salt could influence some of the above mentioned relationships, the chemical structures of the networks suggest they would not form interactions with the salt components. It is also important to note that the enhanced toughness in solution observed in this study is only representative of the polymer properties at a particular immersion time. In this study, immersion time in PBS was held constant (at 1 week) to allow each network to reach its swelling equilibrium, but this time point does not necessarily correspond to the complete stabilization of water–polymer interactions. Studies with PMMA have shown that plasticization will continuously occur well over a month [45]. Therefore because long term mechanical stability is important in many biomedical applications, future studies will examine the effect of varying immersion time over longer durations (i.e. months).

5. Conclusions

Three component (meth)acrylate networks were created to identify relationships between the glass transition region, water behavior, and tensile mechanical properties. One composition within each network was identified as possessing enhanced toughness. Both compositions possessed T_g's close to body temperature, had average elastic moduli values between 50 and 100 MPa in PBS, and exhibited slight PBS absorption (2–3%). The tailoring of T_g to achieve enhanced toughness in the two networks was achieved by two different mechanisms. In the MA-co-MMA-co-PEGDMA network, T_g was adjusted through a copolymer mixing effect and the amount of free water found within the network. The T_g of the 2HEMA-co-BMA-co-PEGDMA network was adjusted by changing the hydrophilicity and subsequently, the total water content of the network. These relationships may be utilized to design photopolymerizable (meth)acrylate networks that will

maintain the needed mechanical properties under aqueous conditions found within the human body.

Acknowledgements

This work was funded by the National Institute of Health (NIAMS; Project# 1806D97). The authors would also like to thank Lex Nunnery for his assistance with thermogravimetric analysis and Dr. Robert Braga in the Department of Chemistry for allowing the use of the FTIR.

References

[1] Myung D, Koh WU, Ko JM, Hu Y, Carrasco M, Noolandi J, et al. Polymer 2007;48(18):5376–87.
[2] Tanaka Y, Gong JP, Osada Y. Progress in Polymer Science 2005;30(1):1–9.
[3] Yakacki CM, Shandas R, Safranski D, Ortega AM, Sassaman K, Gall K. Advanced Functional Materials 2008;18(16):2428–35.
[4] Kong HJ, Wong E, Mooney DJ. Macromolecules 2003;36(12):4582–8.
[5] Smith TL. Journal of Polymer Science: Part A 1965;1:3597–615.
[6] Smith TL. Polymer Engineering and Science 1965:270.
[7] Smith KE, Temenoff JS, Gall K. Journal of Applied Polymer Science 2009;114(5): 2711–22.
[8] Drummond JL. Journal of Dental Research 2008;87(8):710–9.
[9] Jan C, Grzegorz K. Journal of Materials Science-Materials in Medicine 2005;16(11):1051–60.
[10] Barnes A, Corkhill PH, Tighe BJ. Polymer 1988;29(12):2191–202.
[11] Bolon DA, Lucas GM, Olson DR, Webb KK. Journal of Applied Polymer Science 1980;25(4):543–53.
[12] Yang B, Huang WM, Li C, Li L. Polymer 2006;47(4):1348–56.
[13] Hamouda AMS. Journal of Materials Processing and Technology 2002;124:238–43.
[14] Corkhill PH, Jolly AM, Ng CO, Tighe BJ. Polymer 1987;28(10):1758–66.
[15] Hatakeyama T, Nakamura K, Hatakeyama H. Thermochimica Acta 1988;123:153–61.
[16] Yang B, Huang WM, Li C, Lee CM, Li L. Smart Materials & Structures 2004;13(1):191–5.
[17] Hofer K, Mayer E, Johari GP. Journal of Physical Chemistry 1990;94(6):2689–96.
[18] Nakamura K, Hatakeyama T, Hatakeyama H. Polymer 1983;24(7):871–6.
[19] Rault J, Lucas A, Neffati R, Pradas MM. Macromolecules 1997;30(25):7866–73.
[20] Singh TRR, McCarron PA, Woolfson AD, Donnelly RF. European Polymer Journal 2009;45(4):1239–49.
[21] Elisseeff J, Anseth K, Sims D, McIntosh W, Randolph M, Langer R. Proceedings of the National Academy of Sciences of the United States of America 1999;96(6):3104–7.
[22] Yakacki CM, Shandas R, Lanning C, Rech B, Eckstein A, Gall K. Biomaterials 2007;28(14):2255–63.
[23] West JL, Hubbell JA. Reactive Polymers 1995;25(2–3):139–47.
[24] Gall K, Yakacki CM, Liu YP, Shandas R, Willett N, Anseth KS. Journal of Biomedical Materials Research Part A 2005;73A(3):339–48.
[25] Garcia RM, Bartolome MLA, Alvarez AE. Thermochimica Acta 1993;215:281–9.
[26] Rahman MS, Al-Marhubi IM, Al-Mahrouqi A. Chemical Physics Letters 2007;440(4–6):372–7.
[27] Pradas MM, Ribelles JLG, Aroca AS, Ferrer GG, Anton JS, Pissis P. Colloid and Polymer Science 2001;279(4):323–30.
[28] Sanchez MS, Ferrer GG, Pradas MM, Ribelles JLG. Macromolecules 2003;36(3):860–6.
[29] Kusanagi H, Yukawa S. Polymer 1994;35(26):5637–40.
[30] Li XM, Cui YD, Xiao JL, Lia LW. Journal of Applied Polymer Science 2008;108(6):3713–9.
[31] Wang YJ, Tan GX, Zhang SJ, Guang YX. Influence of water states in hydrogels on the transmissibility and permeability of oxygen in contact lens materials. Elsevier Science Bv; 2008. p. 604–6.
[32] Safranski DL, Gall K. Polymer 2008;49(20):4446–55.
[33] Pinal R. Entropy 2008;10(3):207–23.
[34] Pimbert S, Avignon-Poquillon L, Levesque G. Relations between glass transition temperatures in miscible polymer blends and composition: from volume to mass fractions. Wiley-VCH Verlag Gmbh; 2005. p. 259–63.
[35] Gordon M, Taylor J. Journal of Applied Chemistry 1952;2:493–500.
[36] Couchman PR, Karaz FE. Macromolecules 1978;11:117–9.
[37] Sanchez MS, Hanykova L, Ilavsky M, Pradas MM. Polymer 2004;45(12): 4087–94.
[38] Nakamura K, Hatakeyama T, Hatakeyama H. Textile Research Journal 1983;53(11):682–8.
[39] Blasi P, D'Souza SS, Selmin F, DeLuca PP. Journal of Controlled Release 2005;108(1):1–9.
[40] Sutandar P, Ahn DJ, Franses EI. Macromolecules 1994;27(25):7316–28.
[41] Millar JR, Kressman TR, Smith DG, Marr WE. Journal of the Chemical Society 1963(jan):218.
[42] Lustig SR, Caruthers JM, Peppas NA. Polymer 1991;32(18):3340–53.
[43] Refojo MF, Yasuda H. Journal of Applied Polymer Science 1965;9(7):2425.
[44] Blevins FT, Hecker AT, Bigler GT, Boland AL, Hayes WC. American Journal of Sports Medicine 1994;22(3):328–33.
[45] Kusy RP, Whitley JQ, Kalachandra S. Polymer 2001;42(6):2585–95.